Am J Cancer Res 2025;15(8):3486-3499
www.ajcr.us /ISSN:2156-6976/ajcr0164367

Original Article

Study on serum tRF-30-RRJ8909NF5W8 as a potential biomarker for clinical diagnosis of gastric cancer

Zhihan Zhang[1,2], Chunyan Mao[1,2], Yi Wu[1,2], Yin Wang[1,2], Hui Cong[1,3]

[1]Department of Laboratory Medicine, Affiliated Hospital of Nantong University, Nantong 226001, Jiangsu, P. R. China; [2]Department of Clinical Medicine, Medical School of Nantong University, Nantong 226001, Jiangsu, P. R. China; [3]Department of Blood Transfusion, Affiliated Hospital of Nantong University, Nantong 226001, Jiangsu, P. R. China

Received March 6, 2025; Accepted August 12, 2025; Epub August 15, 2025; Published August 30, 2025

Abstract: Gastric cancer (GC) is one of the leading causes of cancer-related deaths worldwide. In this study, our objective was to identify a specific tRNA-derived small RNA (tsRNA) as a biomarker for GC. We developed and validated a methodology to detect the expression level of tRF-30-RRJ8909NF5W8 in the serum of GC patients. The results showed that the expression of tRF-30-RRJ8909NF5W8 was significantly downregulated in the serum of GC patients and increased after radical surgery. Clinicopathological correlation analysis revealed that its expression level was closely associated with TNM stage, T stage, and neural/vascular invasion. Compared with existing GC diagnostic markers, tRF-30-RRJ8909NF5W8 demonstrated superior diagnostic performance, effectively distinguishing GC patients from those with gastritis and healthy controls. These findings suggest that tRF-30-RRJ8909NF5W8 may serve as a promising candidate diagnostic biomarker for GC and provide theoretical support for its potential as a therapeutic target.

Keywords: Gastric cancer, tRNA-derived small RNA, tRF-30-RRJ8909NF5W8, biomarker, diagnosis

Introduction

Gastric cancer represents the fifth most prevalent cancer globally and is the third leading cause of cancer-related mortality [1, 2]. Contributory factors for this malignancy encompass Helicobacter pylori infection, advancing age, elevated salt consumption, and a diet deficient in fruits and vegetables [3]. In recent decades, there has been a notable increase in the emphasis on the detection of Helicobacter pylori, concomitant with an overall decline in the incidence and prevalence of gastric cancer. The primary diagnostic approach for gastric cancer involves endoscopic resection, with histological diagnosis performed following endoscopic biopsy, while staging employs computed tomography (CT), endoscopic ultrasound, positron emission tomography (PET), and laparoscopy [4]. Early-stage gastric cancer typically presents with subtle symptoms, complicating its detection; consequently, this expensive and invasive upper gastrointestinal endoscopy is infrequently utilized during the initial stages [5]. Furthermore, traditional biomarkers such as carcinoembryonic antigen (CEA), carbohydrate antigen (CA-199), and CA-724 are applicable for examination; however, their positive rates and sensitivity remain suboptimal, thus necessitating the urgent identification of new biomarkers characterized by heightened specificity and sensitivity.

Recent advancements in high-throughput sequencing technologies have elucidated that certain DNA fragments generate non-coding RNA, which does not translate into proteins [6]. Historically, such non-protein coding RNAs were labeled as genetic “junk” and deemed devoid of functional significance. The Encyclopedia of DNA Elements (ENCODE) transcriptome project determined that non-coding RNA constitutes a substantial fraction of nucleic acids, with merely 1.2% of the genome containing protein-coding genes, while approximately 80% of the genome is actively transcribed into diverse non-

https://doi.org/10.62347/AIID7730

coding RNAs [7]. Based on their length, non-coding RNAs can be categorized into small non-coding RNA (ncRNA) and long non-coding RNAs (lncRNAs), including microRNAs (miRNAs), circular RNAs (circRNAs), transfer-derived small RNA (tsRNAs), and piwi-interacting non-coding RNAs (piwiRNAs) [8].

tsRNAs is classified as a small RNA derived from tRNAs, which is ubiquitously present in the transcriptomes of both eukaryotic and prokaryotic organisms [9]. tRNAs primarily functions in the transport of amino acids for protein synthesis and is transcribed by RNA polymerase III into precursor tRNAs, subsequently undergoing a series of modifications to yield mature tRNAs. Structurally, tRNAs exhibits a highly folded four-leaf clover configuration, comprising four arms and three loops [10]. tsRNAs can be divided into two principal categories: tRNA-derived fragments (tRFs) and tRNA-derived stress-induced RNAs (tiRNAs) [11]. tRFs are generated through the cleavage of mature tRNAs by Dicer in the cytoplasm, whereas tiRNAs arise from the gradual accumulation of ANG from the nucleus to the cytoplasm. Notably, certain studies have identified the presence of a specific subset of tsRNA within mitochondria, referred to as mt-tRNA, highlighting an additional avenue for comprehensively understanding the mechanisms underlying tsRNAs [12]. Depending on the cleavage site and biogenesis, tRFs can be categorized into four primary isoforms: tRF-1, tRF-3, tRF-5, and i-tRF [10]. Numerous experimental investigations have substantiated the involvement of tsRNAs dysregulation in tumorigenesis. For instance, Lan et al. identified tRF-18-8R6546D2 as a novel biomarker for pancreatic cancer [13]. Fang et al. demonstrated that tsRNA-5001a promotes the proliferation of lung adenocarcinoma cells and is associated with the prognosis of patients diagnosed with lung adenocarcinoma [14]. Additionally, tiRNA-Gly is notably upregulated in papillary thyroid carcinoma (PTC), wherein it directly interacts with RBM17 and exhibits oncogenic effects via RBM17-mediated alternative splicing, with ectopic expression of tiRNA-Gly facilitating cellular proliferation and migration [15].

Materials and methods

Clinical samples

All serum samples in this study, including 107 GC patients, 70 healthy blood donors, 35 gastritis patients, and 27 postoperative GC patients, were obtained from the Department of Laboratory Medicine, Affiliated Hospital of Nantong University, between 2022 and 2024. All collected samples were immediately stored in a -80°C freezer to ensure sample quality. In this study, gastritis patients were diagnosed by clinicians, while GC patients were diagnosed by two or more pathologists and had not received preoperative radiotherapy, chemotherapy, or targeted therapy. This study adhered to the Declaration of Helsinki, ensuring the protection of all participants through voluntary informed consent. The project was approved by the Ethics Committee of the Affiliated Hospital of Nantong University (Ethics Review Report No. 2023-K167-01).

Cell culture

We purchased human GC cell lines (HGC-27, BGC-823, AGS) and normal human gastric epithelial cells (GES-1) from the Shanghai Institute of Biological Sciences, Chinese Academy of Sciences (Shanghai, China). HGC-27 and BGC-823 cells were cultured in RPMI-1640 medium containing 10% fetal bovine serum (FBS) (Gibco, USA) and 1% penicillin-streptomycin (XinXibao, Suzhou, China). AGS cells were cultured in an AGS-specific medium and incubated at 37°C in an incubator with 5% CO_2.

RNA extraction and Real-Time Quantitative Polymerase Chain Reaction (RT-qPCR)

Total RNA from serum samples was extracted using the Rapid Blood Total RNA Extraction Kit (BioTeke, Wuxi, China), while total RNA from cells was extracted using the RNA-Easy Isolation Reagent (Vazyme, Nanjing, China). tRF-30-RRJ89O9NF5W8 was used as the target molecule, with RNU6B as the internal reference. The RevertAid RT Reverse Transcription Kit (Thermo Fisher Scientific, USA) and specific primers (Ribobio, Guangzhou, China) were used to generate 10 μL cDNA, including tRF-30-RRJ89O9NF5W8 RT and RNU6B RT. The prepared 10 μL mixture was amplified at 42°C for 1 hour, then inactivated at 70°C for 5 minutes, and stored at either 4°C for short-term use -20°C for long-term storage. Next, real-time quantitative PCR was performed using the ABI QuantStudio 5 system with a 20 μL reaction system composed of 10 μL ChamQ Universal SYBR qPCR Master Mix (Vazyme Biotech Co.,

Ltd., China), 5 μL cDNA, 1 μL forward primer, 1 μL reverse primer (Ribobio, Guangzhou, China), and 3 μL nuclease-free water. The expression levels of tRF-30-RRJ89O9NF5W8 were calculated using the 2^−ΔΔCT method, with the formula: ΔCT = Ct (target) - Ct (reference) ΔΔCT = ΔCT (experimental group) - ΔCT (control group) All procedures were performed according to the manufacturer's instructions.

Gradient dilution experiment

RNA was extracted from a randomly mixed set of 20 serum samples and used to synthesize cDNA, which was then serially diluted 10×, 100×, 1,000×, 10,000×, and 100,000×.

Room temperature and freeze-thaw stability experiment

A randomly mixed set of 20 serum samples was used. Some mixed serum samples were incubated at room temperature (25°C) for 0, 6, 12, 18, and 24 hours. Additionally, other mixed serum samples were repeatedly frozen and thawed at -80°C and room temperature for 0, 1, 3, 5, and 10 cycles. RNA was then extracted and analyzed for tRF-30-RRJ89O9NF5W8 expression using RT-qPCR.

Nuclear and cytoplasmic RNA separation assay

Cultured BGC-823 and AGS cells were digested with trypsin and collected in 1.5 mL EP tubes once the cell count reached 5 × 10^6. The Nuclear and Cytoplasmic Protein Extraction Kit (Beyotime, China) was used to extract 60 μL of nuclear and cytoplasmic RNA, which was subsequently stored at -80°C.

Statistical analysis

Statistical analyses were performed using SPSS version 26.0 (IBM SPSS Statistics, Chicago, USA) and GraphPad Prism v10.2 (GraphPad Software, San Diego, California, USA). The relative expression levels of tRF-30-RRJ89O9NF5W8 in each group are reported as mean ± standard deviation (SD). The Wilcoxon matched-pairs signed-rank test was used to analyze the expression levels of tRF-30-RRJ89O9NF5W8 in preoperative and postoperative serum samples from gastric cancer (GC) patients. An independent-samples t-test was used to compare two independent groups, as well as GC tissues and their matched adjacent normal tissues. One-way analysis of variance (ANOVA) was performed to compare the expression levels of tRF-30-RRJ89O9NF5W8 among multiple groups. The chi-square test in SPSS version 26.0 was used to evaluate the correlation between tRF-30-RRJ89O9NF5W8 expression and clinicopathological parameters. Receiver operating characteristic (ROC) curves and the area under the curve (AUC) were generated and calculated to assess the diagnostic performance of serum tRF-30-RRJ89O9NF5W8 for GC. The cutoff value was determined using the Youden index and ROC curve analysis. Based on the reference ranges from the Affiliated Hospital of Nantong University, the cutoff values for CEA, CA-199, and CA-724 were set at 5 ng/mL, 37 U/mL, and 10 U/mL, respectively. A *P*-value < 0.05 was considered statistically significant.

Results

Database screening, structure, and origin of tsRNA-Gln-5-0033

Based on the criteria of a *p*-value < 0.05 and $|\log_2$ (fold change)| > 2d3, three tsRNAs were selected using the tsRFun database (https://rna.sysu.edu.cn/tsRFun/index): tsRNA-Gln-5-0033, tsRNA-Arg-i-0254, and tsRNA-iMet-i-0014. Subsequently, we collected serum samples from 20 gastric cancer (GC) patients and 20 healthy individuals to assess the expression levels of these tsRNAs (**Figure 1A-C**). Among them, tsRNA-Gln-5-0033 exhibited the lowest expression. To further validate the consistency of tsRNA-Gln-5-0033 expression, we collected paired gastric cancer and adjacent non-tumor tissues from another 20 GC patients (**Figure 1D**) and found that the expression level of tRF-30-RRJ89O9NF5W8 in tissues was consistent with that observed in serum. Additionally, the melting curves showed specific single peaks, indicating the high stability and reproducibility of the assay (**Figure 1E**). We accessed the UCSC Genome Browser (https://genome-asia.ucsc.edu/) and selected the human genome assembly GRCh38/hg38 to retrieve the basic information of tRF-30-RRJ89O9NF5W8. It is located on chromosome 6 at q24.3, with coordinates 145,182,723-145,182,752 (**Figure 1F**). Due to the lack of a unified naming system,

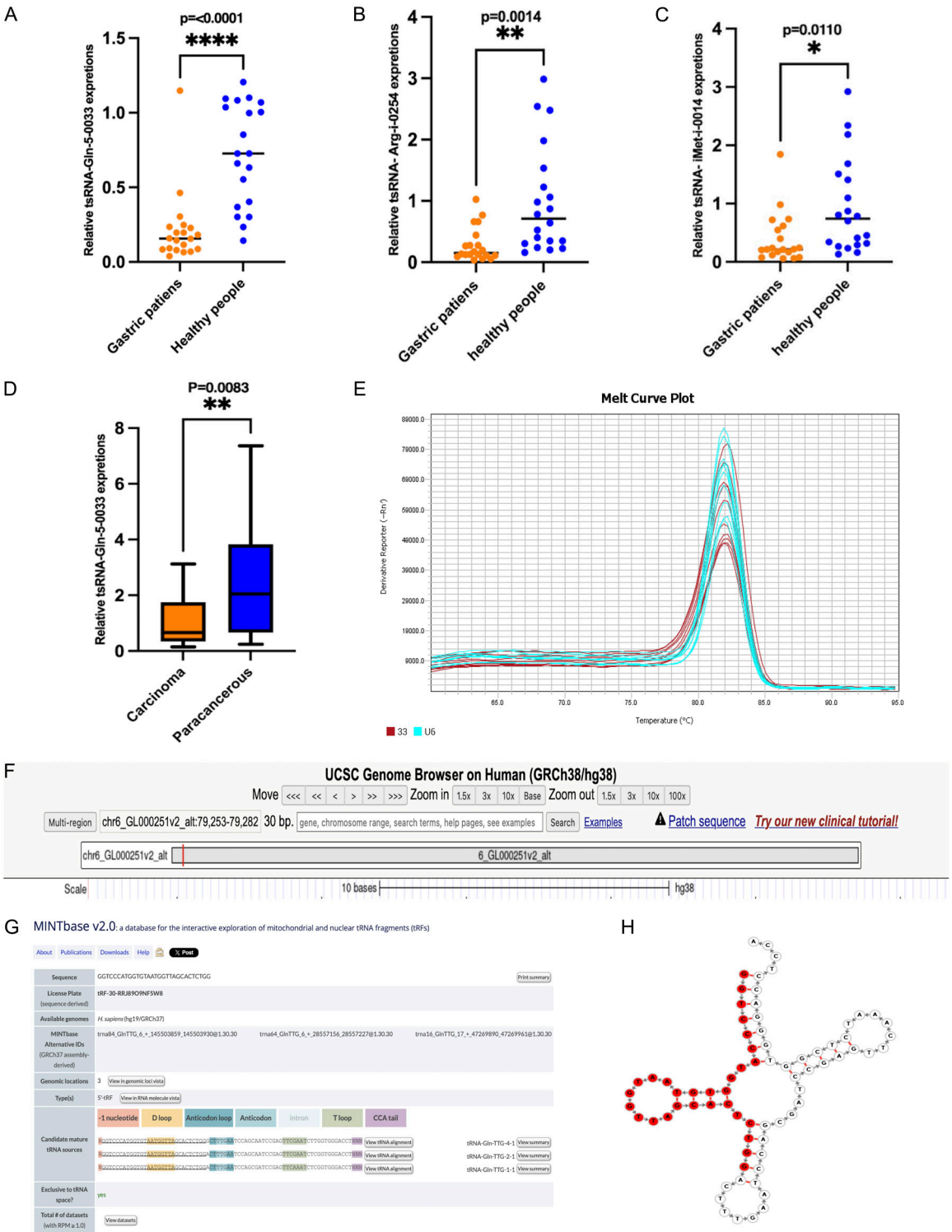

Figure 1. Selection of tsRNA-Gln-5-0033, and its structure and origin. A. Expression level of tsRNA-Gln-5-0033 in the serum of GC (gastric cancer) patients. B. Expression level of tsRNA-Arg-i-0254. C. Expression level of tsRNA-iMet-i-0014. D. Expression level of tsRNA-Gln-5-0033 in 20 paired GC tissues and adjacent non-tumorous tissues. E. The melting curves show distinct single peaks, indicating good stability and reproducibility of the assay. F. tsRNA-Gln-5-0033 is located at chr6, q24.3, coordinates 182,723-182,752. G. tsRNA-Gln-5-0033 is named tRF-30-RRJ8909NF5W8 in MINTbase v2.0, where it is shown to be 30 nucleotides in length (5'-GGTCCCATGGTGTAATGGTTAGCACTCTGG-3'). H. The cleavage site of tRF-30-RRJ8909NF5W8 is located in the tRF-5a and anticodon arm region of the mature tRNA. *P < 0.05; **P < 0.01; ***P < 0.001; ****P < 0.0001.

Table 1. The intra-assay and inter-assay repeatability difference of tRF-30-RRJ89O9N-F5W8

	tRF-30-RRJ89O9NF5W8	U6
Intra-assay CV (%)	1.2	1.3
Inter-assay CV (%)	1.9	2.4

we named it tRF-30-RRJ89O9NF5W8 according to the MINTbase v2.0 database (https://cm.jefferson.edu/MINTbase/).

We confirmed that tRF-30-RRJ89O9NF5W8 is a 30 bp 5'-tRF (5'-GGTCCCATGGTGTAATGGTTAGCACTCTGG-3') derived from tRNA-Gln-TTG. It is cleaved at the junction between the tRF-5a and the anticodon arm of the mature tRNA (**Figure 1G**, **1H**).

Evaluation of serum tRF-30-RRJ89O9NF5W assay

To better verify the stability of tRF-30-RRJ89O9NF5W, a comprehensive evaluation of its measurement was conducted. Additionally, 20 randomly selected serum samples were mixed and allocated into 20 batches, including GC patients and healthy donors. Total RNA was extracted from 10 samples within the same RT-qPCR batch, and Ct values were used to calculate the intra-batch coefficient of variation (CV). The inter-batch CV and intra-batch CV of tRF-30-RRJ89O9NF5W were 1.2% and 1.9%, respectively (**Table 1**), indicating high precision. The 20 mixed serum samples were divided into two groups for RNA extraction and RT-qPCR analysis. One group was stored at room temperature for 0, 6, 12, 18, and 24 hours. The other group underwent repeated freeze-thaw cycles (0, 1, 3, 5, and 10 times). The results of both experiments showed no significant difference in tRF-30-RRJ89O9NF5W expression, $P > 0.05$ (**Figure 2A**, **2B**). Furthermore, gradient dilution experiments showed that: The correlation coefficient (R^2) for tRF-30-RRJ89O9NF5W was 0.9919, with a linear equation of $Y = -2.862*X + 16.72$. The correlation coefficient (R^2) for U6 was 0.9996, with a linear equation of $Y = -3.316*X + 7.487$ (**Figure 2C**, **2D**). Agarose gel electrophoresis confirmed that the RT-qPCR product of tRF-30-RRJ89O9NF5W was approximately 80 bp in size (**Figure 2E**). All results exhibited excellent linear correlation (**Figure 2F**).

Analysis of serum tRF-30-RRJ89O9NF5W8 expression and its correlation with clinicopathological parameters

Investigation of tRF-30-RRJ89O9NF5W8 as a Potential Biomarker for GC Diagnosis. To determine whether tRF-30-RRJ89O9NF5W could serve as a biomarker for GC diagnosis, we evaluated its expression levels in serum samples from 107 GC patients, 70 healthy donors, and 35 gastritis patients using RT-qPCR. The results showed that tRF-30-RRJ89O9NF5W8 expression was significantly lower in GC patients compared to healthy donors and gastritis patients (**Figure 3A**). Moreover, there was no significant difference in tRF-30-RRJ89O9NF5W8 expression between healthy individuals and gastritis patients (**Figure 3B**). By analyzing tRF-30-RRJ89O9NF5W8 expression in 27 postoperative GC patients, we found that its expression increased after surgery, showing no significant difference compared to healthy donors (**Figure 3C**). This suggests that tRF-30-RRJ89O9NF5W8 could be used to monitor postoperative dynamics in GC patients. To explore the correlation between tRF-30-RRJ89O9NF5W8 expression levels and clinicopathological parameters of GC patients, we classified the patients into two groups: The high-expression group: 54 GC patients with expression levels above the median. Low-expression group: Remaining patients with expression levels below the median. Chi-square test results revealed that tRF-30-RRJ89O9NF5W expression was significantly associated with T stage ($P = 0.043$), TNM stage ($P = 0.031$), and neural/vascular invasion ($P = 0.009$). However, no significant correlation was observed with age, sex, tumor size, differentiation grade, lymph node metastasis, Lauren classification, CEA, CA-199, or CA-724 (**Table 2**).

We divided 107 GC patients into two groups based on the median expression level of tRF-30-RRJ89O9NF5W8 in their serum: High-expression group (N = 54). Low-expression group (N = 53). This classification was used to evaluate whether tRF-30-RRJ89O9NF5W8 has clinical value. Chi-square test results showed that tRF-30-RRJ89O9NF5W8 expression levels were not associated with gender, age, tumor size, CEA, CA-199, CA-724, or Lauren classification. However, significant correlations were found with the T stage ($P = 0.043$), tumor

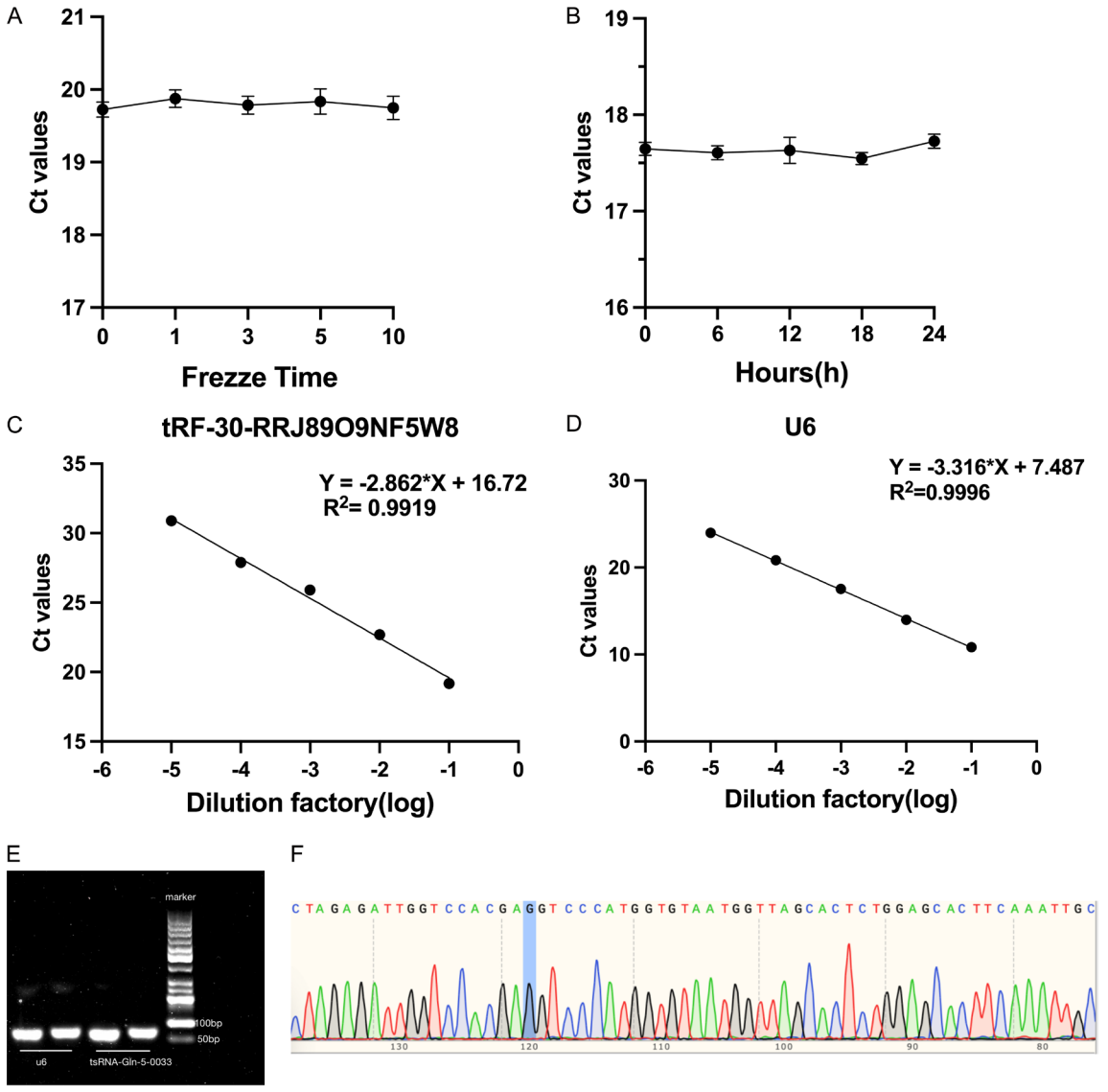

Figure 2. Evaluation of tRF-30-RRJ8909NF5W8 assay. A, B. Room temperature and repeated freeze-thaw experiments showed no significant changes in tRF-30-RRJ8909NF5W8 expression levels. C, D. Standard curves of tRF-30-RRJ8909NF5W8 (R^2 = 0.9919) and U6 (R^2 = 0.9996). E. tRF-30-RRJ8909NF5W8 length (80 bp) was verified by agarose gel electrophoresis. F. Sanger sequencing of the RT-qPCR product confirmed that the product contained the full-length sequence of tRF-30-RRJ8909NF5W8.

metastasis (TNM stage, P = 0.031), and neural/vascular invasion (P = 0.009) (**Table 2**). To further explore these significant clinicopathological parameters, we analyzed tRF-30-RRJ8909NF5W8 expression differences within each subgroup: By analyzing tRF-30-RRJ8909NF5W8 expression in healthy donors and GC patients at different T stages (T1-T4), we observed that expression levels decreased as tumor invasion depth increased (**Figure 3D**). Based on TNM staging, we categorized GC patients into stage I-II and stage III-IV. The results showed that tRF-30-RRJ8909NF5W8 expression in both stages was significantly lower than in healthy donors (**Figure 3E**). GC patients with vascular/neural invasion exhibited significantly lower tRF-30-RRJ8909NF5W8 expression compared to those without invasion (**Figure 3F**). These findings suggest that tRF-30-RRJ8909NF5W8 has potential value in monitoring the progression of gastric malignancies.

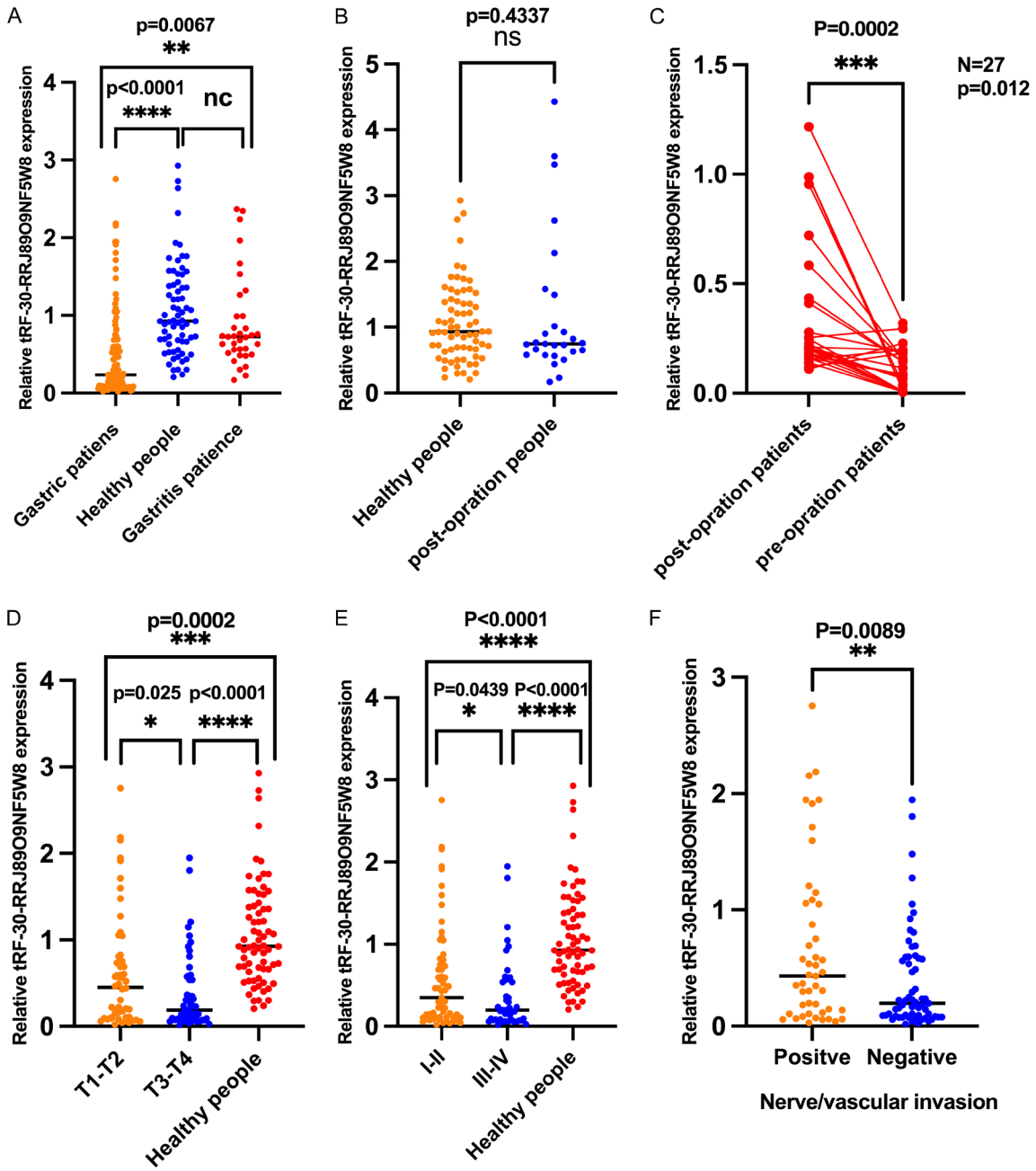

Figure 3. Clinical value of tRF-30-RRJ89O9NF5W8 in GC serum. A. Expression levels of tRF-30-RRJ89O9NF5W8 in serum samples from GC patients (n = 107), gastritis patients (n = 35), and healthy donors (n = 70). B. Differences in tRF-30-RRJ89O9NF5W8 expression levels in serum samples from postoperative GC patients and healthy donors. C. Changes in serum tRF-30-RRJ89O9NF5W8 expression levels in 27 GC patients before and after surgery. D. Expression levels of tRF-30-RRJ89O9NF5W8 in different stages of tumor invasion depth compared to healthy donors (T1-T2: n = 54, T3-T4: n = 53, healthy donors: n = 70). E. Serum tRF-30-RRJ89O9NF5W8 expression levels in GC patients at stages I-II (n = 59), stages III-IV (n = 48), and healthy donors (n = 70). F. Expression levels of tRF-30-RRJ89O9NF5W8 in the serum of GC patients with (n = 46) or without (n = 61) neural/vascular invasion. $^{*}P < 0.05$; $^{**}P < 0.01$; $^{***}P < 0.001$; $^{****}P < 0.0001$.

Diagnostic value of tRF-30-RRJ89O9NF5W8 in GC serum

Evaluation of the Diagnostic Value of tRF-30-RRJ89O9NF5W8 in GC Serum, to assess the diagnostic value of tRF-30-RRJ89O9NF5W8 in GC serum, we performed ROC analysis on tRF-30-RRJ89O9NF5W8, CEA, CA-199, and CA-724. The results showed that: tRF-30-RRJ89O9NF5W8 had an AUC of 0.803 (95% CI:

Table 2. Clinicopathological analysis of tRF-30-RRJ8909NF5W8

Parameter	n	tRF-RRJ8909NF5W8 (low)	tRF-RRJ8909NF5W8 (high)	*P* value
Sex				
Male	23	13	10	0.391
Femle	84	39	45	
Age				
< 60	25	12	13	0.946
≥ 60	82	40	42	
Tumor size				
< 5	77	35	42	0.297
≥ 5	30	17	13	
Differentiation grade				
Well differentiatiated	22	12	10	0.531
Poorly differentiated	85	40	45	
T stage				
T1-T2	54	21	33	0.043*
T3-T4	53	31	22	
Lymph node status				
Positive	59	32	27	0.196
Negative	48	20	28	
TNM stage				
I-II	59	27	32	0.031*
III-IV	48	32	16	
Nerve/vascular invasion				
Positive	46	29	17	0.009***
Negative	61	23	38	
Lauren classification				
Intestinal type	55	22	33	0.537
Mixed type	28	16	12	
Diffuse type	29	14	15	
CEA				
< 5	80	36	44	0.200
≥ 5	27	16	11	
CA-199				
< 37.0	84	40	44	0.699
≥ 37.0	23	12	11	
CA-724				
< 10.0	83	37	46	0.122
≥ 10.0	24	15	9	

*P < 0.05; ***P < 0.001.

0.740-0.867), higher than CEA (AUC = 0.771, 95% CI: 0.702-0.840), CA-199 (AUC = 0.570, 95% CI: 0.487-0.654), CA-724 (AUC = 0.550, 95% CI: 0.464-0.637), indicating that tRF-30-RRJ8909NF5W8 exhibits good diagnostic performance in GC serum (**Figure 4A**). Furthermore, SPSS analysis determined a cutoff value of 0.62, with a corresponding Youden index of 0.456. The diagnostic performance of tRF-30-RRJ8909NF5W8 was as follows: Sensitivity (SEN): 74.76%, Specificity (SPE): 77.14%, Overall accuracy (AUUC): 75.70%, Positive predictive value (PPV): 83.33%, Negative predictive value (NPV): 66.67%, Overall, tRF-30-RRJ8909NF5W8 outperformed CEA, CA-199, and CA-724, suggesting that serum tRF-30-RRJ8909NF5W8 can effectively distinguish GC patients from healthy donors. Addi-

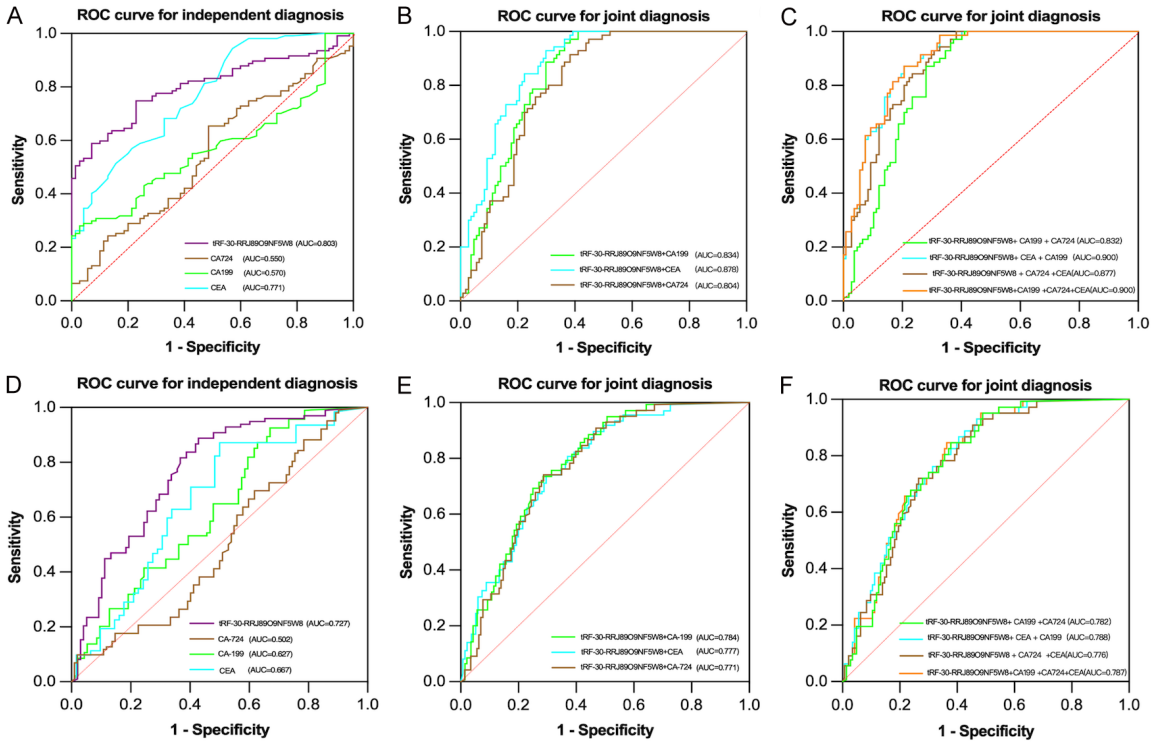

Figure 4. Diagnostic value of tRF-30-RRJ8909NF5W8 in GC serum. A-C. ROC curves for independent diagnosis and joint diagnosis of tRF-30-RRJ8909NF5W8, CEA, CA199, and CA724 in differentiating GC patients from healthy donors. D-F. ROC curves for independent diagnosis and joint diagnosis of tRF-30-RRJ8909NF5W8, CEA, CA199, and CA724 in differentiating GC patients from gastritis patients.

tionally, we found that combining serum tRF-30-RRJ8909NF5W8 with CEA, CA-199, and CA-724 improved diagnostic performance more than any single biomarker. The combined four-biomarker panel achieved a maximum sensitivity of 82.84%, further enhancing the diagnostic effectiveness of tRF-30-RRJ8909NF5W8 (**Figure 4B**, **4C**; **Table 3**).

Studies have shown that chronic gastritis and GC share similar early symptoms, making them difficult to distinguish. Therefore, identifying biomarkers that differentiate gastritis from GC is crucial. We conducted ROC analysis on 107 GC patients and 35 gastritis patients and found that: tRF-30-RRJ8909NF5W8 had an AUC of 0.727 (95% CI: 0.700-0.833), Higher than CEA (AUC = 0.667, 95% CI: 0.564-0.758), CA-199 (AUC = 0.627, 95% CI: 0.547-0.707), CA-724 (AUC = 0.502, 95% CI: 0.421-0.582) (**Figure 4D**). When the cutoff value was set at 0.4714 with a Youden index of 0.483, tRF-30-RRJ8909NF5W8 demonstrated a sensitivity (SEN) of 62.62% for differentiating GC from gastritis patients. ACCU (67.83%) and NPV (42.86%) were also higher than those of CEA, CA-199, and CA-724 (**Table 4**). When tRF-30-RRJ8909NF5W8 was combined with other markers, the AUC further increased (**Figure 4E**, **4F**), reaching 0.787. Additionally, when all four GC markers were combined, the sensitivity increased to 76.63% (**Table 4**). In conclusion, tRF-30-RRJ8909NF5W8 is a promising biomarker for distinguishing gastritis from GC.

Downstream forecast for tRF-30-RRJ8909NF5W8

We used nuclear and cytoplasmic RNA fractionation to visualize the distribution of tRF-30-RRJ8909NF5W8 in BGC-823 and AGS cells, revealing that tRF-30-RRJ8909NF5W8 is primarily localized in the cytoplasm (**Figure 5A**). This finding provides a general direction for our subsequent experiments. Next, we utilized the miRanda, RNAhybrid, and TargetScan databases to identify potential target sites of tRF-30-RRJ8909NF5W8. The network diagram displayed 640 common target genes across all three databases (**Figure 5B**), laying the foun-

Table 3. Evaluation of the diagnostic value of tRF-30-RRJ8909NF5W8, CEA, CA199, CA-724 and combinations for GC patients and healthy donors

	SEN (%)	SPE (%)	AUUC (%)	PPV (%)	NPV (%)
tRF-30-RRJ8909NF5W8	74.76 (80/107)	77.14 (54/70)	75.70 (134/177)	83.33 (80/96)	66.67 (54/81)
CEA	25.23 (27/107)	98.57 (69/70)	54.23 (96/177)	96.42 (27/28)	46.30 (69/149)
CA-199	21.50 (23/107)	100 (70/70)	52.54 (93/177)	100 (23/23)	45.45 (70/154)
CA-724	22.43 (24/107)	87.14 (61/70)	48.02 (85/177)	72.73 (24/33)	42.36 (61/144)
tRF-30-RRJ8909NF5W8+CEA	77.57 (83/107)	75.71 (53/70)	76.84 (136/177)	83.00 (83/100)	68.83 (53/77)
tRF-30-RRJ8909NF5W8+CA199	78.50 (84/107)	77.14 (54/70)	77.97 (138/177)	84.00 (84/100)	70.12 (54/77)
tRF-30-RRJ8909NF5W8+CA724	75.70 (81/107)	64.29 (45/70)	71.19 (136/177)	76.42 (81/106)	63.38 (45/71)
tRF-30RRJ8909NF5W8+CEA+CA199	81.30 (81/107)	75.71 (53/70)	79.10 (140/177)	83.65 (83/104)	72.60 (53/73)
tRF-30RRJ8909NF5W8+CEA+CA724	78.50 (84/107)	62.86 (44/70)	72.32 (128/177)	76.36 (84/110)	65.67 (44/67)
tRF-30RRJ8909NF5W8+CEA+CA199+CA724	82.24 (88/107)	62.86 (44/70)	74.58 (132/177)	77.19 (88/114)	69.84 (44/63)

SEN, sensitivity; SPE, specificity; ACCU, overall accuracy; PPV, positive predictive value; NPV, negative predictive value.

Table 4. Evaluation of the diagnostic value of tRF-30-RRJ8909NF5W8, CEA, CA199, CA724 and combinations for GC patients and gastritis patients

	SEN (%)	SPE (%)	AUUC (%)	PPV (%)	NPV (%)
tRF-30-RRJ8909NF5W8	62.62 (67/107)	85.71 (30/35)	67.83 (97/142)	93.05 (67/72)	42.86 (30/70)
CEA	25.23 (27/107)	94.28 (33/35)	42.25 (60/142)	93.10 (27/29)	29.20 (33/113)
CA199	21.50 (23/107)	97.14 (34/35)	40.14 (57/142)	95.83 (23/24)	28.81 (34/118)
CA724	20.56 (22/107)	88.57 (31/35)	37.32 (53/142)	84.62 (22/26)	26.72 (31/116)
tRF-30-RRJ8909NF5W8+CEA	81.30 (87/107)	77.14 (27/35)	80.28 (114/142)	91.57 (87/95)	57.45 (27/47)
tRF-30-RRJ8909NF5W8+CA199	67.28 (72/107)	80.00 (28/35)	70.42 (100/142)	91.14 (72/79)	44.44 (28/63)
tRF-30-RRJ8909NF5W8+CA724	65.42 (70/107)	71.43 (25/35)	66.90 (95/142)	87.50 (70/80)	40.32 (25/62)
tRF-30RRJ8909NF5W8+CEA+CA199	73.83 (79/107)	77.14 (27/35)	74.65 (106/142)	90.80 (79/87)	49.09 (27/55)
tRF-30RRJ8909NF5W8+CEA+CA724	71.96 (77/107)	68.57 (24/35)	71.13 (101/142)	87.50 (77/88)	44.44 (24/54)
tRF-30RRJ8909NF5W8+CEA+CA199+CA724	76.63 (82/107)	65.71 (23/35)	73.94 (105/142)	87.23 (82/94)	47.92 (23/48)

SEN, sensitivity; SPE, specificity; ACCU, overall accuracy; PPV, positive predictive value; NPV, negative predictive value.

dation for further exploration of tRF-30-RRJ-8909NF5W8's functional mechanisms. According to Gene Ontology (GO) enrichment analysis (**Figure 5C**), the predicted target genes may be involved in: Postsynaptic cytosol, Anchored components of the synaptic membrane, Inositol 1,4,5-trisphosphate binding. Additionally, the Kyoto Encyclopedia of Genes and Genomes (KEGG) pathway enrichment analysis revealed that these genes are enriched in: Endocytosis, Calcium signaling pathway, and Proteoglycans in cancer (**Figure 5D**). These findings provide new insights into the molecular mechanisms of tRF-30-RRJ8909NF5W8 in GC.

Discussion

Gastric cancer (GC) is one of the most prevalent and lethal malignancies worldwide, particularly in East Asia (e.g., China, Japan, and South Korea) [16]. Although progress has been made in the diagnosis and treatment of GC, many patients are diagnosed at advanced stages due to the absence of early symptoms, leading to poor treatment outcomes [17]. Therefore, identifying novel biomarkers and therapeutic targets is crucial for early diagnosis and precision therapy. Current diagnostic methods for GC are often invasive and costly, making early detection challenging. In recent years, tRNA-derived small RNAs (tsRNAs), a novel class of non-coding RNAs, have attracted attention for their role in GC pathogenesis, progression, and treatment [18]. Research has shown that tsRNAs participate in multiple biological processes, including cell proliferation, migration, cancer progression [19, 20], DNA damage repair [21], sperm modification [22], and epigenetic regulation [23]. Moreover, tsRNAs have been implicated in cancer diagnosis and prognosis prediction [24]. For instance, tsRNA-Thr-5-0015 is significantly elevated in the serum of hepatocellular carcinoma (HCC) patients compared to hepatitis cases and healthy individuals. It is associated with TNM stage and lymph node metastasis and can serve as a novel biomarker

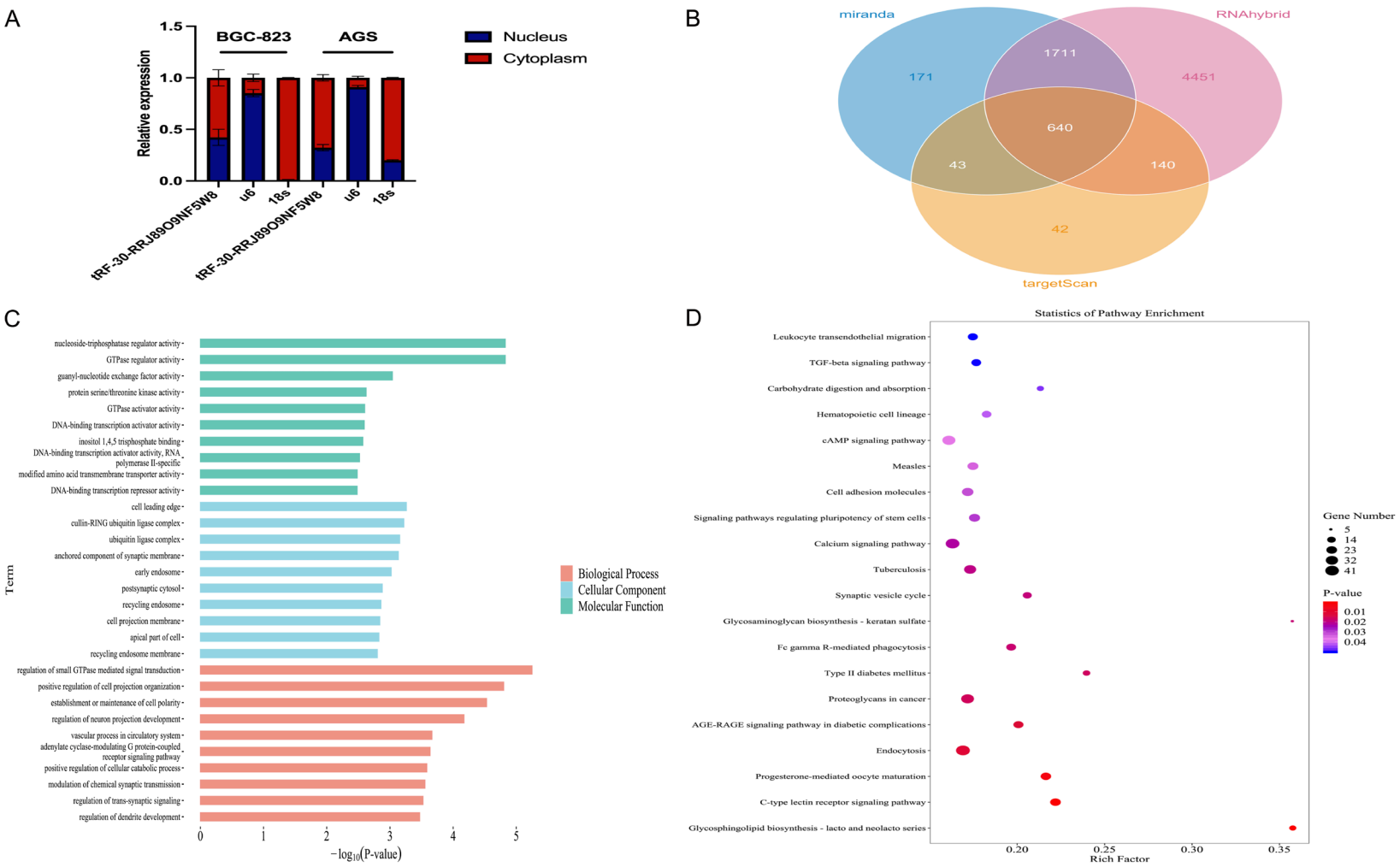

Figure 5. tRF-30-RRJ8909NF5W8 downstream regulation mechanism. A. Nuclear and Cytoplasmic RNA Separation Assay was performed on BGC-823 and AGS for the detection of tRF-30-RRJ8909NF5W8. B. The potential target genes of tRF-30-RRJ8909NF5W8. C. Functional enrichment analysis of GO of tRF-30-RRJ8909NF5W8 potential target genes. D. Enrichment analysis of the KEGG biological pathway of tRF-30-RRJ8909NF5W8 potential target genes.

for HCC [25]. Additionally, tRF-Val-CAC-016 was found to be downregulated in GC, and its overexpression inhibited GC cell proliferation. Xu et al. [26] demonstrated that tRF-Val-CAC-016 regulates the MAPK signaling pathway by targeting CACNA1D. Despite existing challenges, the growing research on tsRNAs and advancements in technology suggest a promising future for tsRNAs in disease diagnosis and treatment.

In this study, we screened a differentially expressed tsRNA, tsRNA-Gln-5-0033, from the tsRFun database and named it tRF-30-RRJ89O9NF5W8 based on MINTbase v2.0. We confirmed that tRF-30-RRJ89O9NF5W8 was consistently downregulated in GC cells and serum samples. Assay evaluations demonstrated its stability, precision, and reliability, laying the foundation for further investigations. Expression analysis revealed that tRF-30-RRJ89O9NF5W8 could distinguish GC patients from healthy donors and gastritis patients. Postoperative GC patients exhibited increased tRF-30-RRJ89O9NF5W8 levels, with no significant difference compared to healthy donors, suggesting its potential role as a tumor suppressor. tRF-30-RRJ89O9NF5W8 levels were significantly correlated with the T stage, TNM stage, and neural/vascular invasion, indicating its involvement in GC progression. Traditional GC biomarkers such as CEA, CA-199, and CA-724 have limited diagnostic efficiency, making early GC detection difficult. Notably, ROC analysis showed that tRF-30-RRJ89O9NF5W8 outperformed CEA, CA-199, and CA-724 in diagnostic accuracy. Moreover, combining tRF-30-RRJ89O9NF5W8 with these biomarkers further enhanced diagnostic performance, suggesting its potential in GC detection and disease monitoring.

Although our findings provide valuable insights, several limitations remain: The mechanisms underlying the dysregulated expression of tRF-30-RRJ89O9NF5W8 remain unclear, tsRNAs can interact with various proteins, contributing to cancer progression. For instance: tRF-33-P4R8YP9LON4VDP binds to AGO2, downregulating STAT3 expression, thereby inhibiting GC tumorigenesis [27], tiRNA-Val-CAC-2 interacts with FUBP1, enhancing its stability and increasing c-MYC transcription, leading to pancreatic cancer metastasis [28]. 5'tiRNA-His-GTG, a stress-induced tsRNA, promotes colorectal cancer progression under hypoxic conditions via the HIF1α/angiogenin (ANG) axis, inhibiting apoptosis and enhancing malignancy [29]. RNA modifications also play a critical role in regulating cellular processes [30]: 5'tsRNA-GlyGCC, upregulated in colorectal cancer (CRC), is modified by METTL1-mediated N^7-methylguanosine (m^7G) tRNA methylation. It activates the JAK1/STAT6 pathway via SPIB targeting, promoting CRC progression [31]. m^7G-3'-tiRNA LysTTT (mtiRL) interacts with ANXA2, enhancing Yes1 phosphorylation and promoting bladder cancer metastasis [32]. Given these findings, we will further investigate the downstream mechanisms of tRF-30-RRJ89O9NF5W8. Using bioinformatics predictions, we identified potential target genes and performed GO and KEGG enrichment analyses, which will guide future research into its regulatory pathways.

Conclusion

In summary, this study identified tRF-30-RRJ89O9NF5W8 as a novel biomarker for GC, demonstrating the downregulation of tRF-30-RRJ89O9NF5W8 in GC for the first time. Significant differentiation between GC patients, gastritis patients, and healthy donors. Superior diagnostic efficiency compared to traditional markers (CEA, CA-199, CA-724). Postoperative expression recovery suggests potential as a therapeutic target. Moving forward, we will further explore the downstream mechanisms of tRF-30-RRJ89O9NF5W8 to understand its role in GC development and progression.

Acknowledgements

This work was supported by the Key Medical Research Projects of Jiangsu Provincial Health Commission (No. ZD2022008).

Disclosure of conflict of interest

None.

Abbreviations

lncRNAs, Long non-coding RNAs; piwiRNAs, Piwi-interacting RNAs; tRFs, TRNA-derived fragments; SD, Standard deviation; AUC, Area under curve; CV, Coefficient of variation; SEN, Sensitivity; SPE, Specificity; ACCU, The overall accuracy; PPV, Positive predictive value; NPV,

Negative predictive value; CI, Confidence interval; GO, Gene Ontology; KEGG, Kyoto Encyclopedia of Genes and Genomes.

Address correspondence to: Hui Cong, Department of Laboratory Medicine, Affiliated Hospital of Nantong University, 20 Xisi Road, Nantong 226001, Jiangsu, P. R. China. Tel: +86-139-62917928; E-mail: huicjs@163.com; Ch_jyk@ntu.edu.cn

References

[1] Machlowska J, Baj J, Sitarz M, Maciejewski R and Sitarz R. Gastric cancer: epidemiology, risk factors, classification, genomic characteristics and treatment strategies. Int J Mol Sci. 2020; 21: 4012.

[2] Rahman R, Asombang AW and Ibdah JA. Characteristics of gastric cancer in Asia. World J Gastroenterol 2014; 20: 4483-4490.

[3] Gullo I, Grillo F, Mastracci L, Vanoli A, Carneiro F, Saragoni L, Limarzi F, Ferro J, Parente P and Fassan M. Precancerous lesions of the stomach, gastric cancer and hereditary gastric cancer syndromes. Pathologica 2020; 112: 166-185.

[4] Hartgrink HH, Jansen EP, van Grieken NC and van de Velde CJ. Gastric cancer. Lancet 2009; 374: 477-490.

[5] Kim SJ and Choi CW. Common locations of gastric cancer: review of research from the endoscopic submucosal dissection era. J Korean Med Sci 2019; 34: e231.

[6] Slack FJ and Chinnaiyan AM. The role of noncoding RNAs in oncology. Cell 2019; 179: 1033-1055.

[7] ENCODE Project Consortium, Moore JE, Purcaro MJ, Pratt HE, Epstein CB, Shoresh N, Adrian J, Kawli T, Davis CA, Dobin A, Kaul R, Halow J, Van Nostrand EL, Freese P, Gorkin DU, Shen Y, He Y, Mackiewicz M, Pauli-Behn F, Williams BA, Mortazavi A, Keller CA, Zhang XO, Elhajjajy SI, Huey J, Dickel DE, Snetkova V, Wei X, Wang X, Rivera-Mulia JC, Rozowsky J, Zhang J, Chhetri SB, Zhang J, Victorsen A, White KP, Visel A, Yeo GW, Burge CB, Lécuyer E, Gilbert DM, Dekker J, Rinn J, Mendenhall EM, Ecker JR, Kellis M, Klein RJ, Noble WS, Kundaje A, Guigó R, Farnham PJ, Cherry JM, Myers RM, Ren B, Graveley BR, Gerstein MB, Pennacchio LA, Snyder MP, Bernstein BE, Wold B, Hardison RC, Gingeras TR, Stamatoyannopoulos JA and Weng Z. Expanded encyclopaedias of DNA elements in the human and mouse genomes. Nature 2020; 583: 699-710.

[8] Niderla-Bielińska J, Jankowska-Steifer E and Włodarski P. Non-coding RNAs and human diseases: current status and future perspectives. Int J Mol Sci 2023; 24: 11679.

[9] Kim HK, Fuchs G, Wang S, Wei W, Zhang Y, Park H, Roy-Chaudhuri B, Li P, Xu J, Chu K, Zhang F, Chua MS, So S, Zhang QC, Sarnow P and Kay MA. A transfer-RNA-derived small RNA regulates ribosome biogenesis. Nature 2017; 552: 57-62.

[10] Lee S, Kim J, Valdmanis PN and Kim HK. Emerging roles of tRNA-derived small RNAs in cancer biology. Exp Mol Med 2023; 55: 1293-1304.

[11] Chen Q, Zhang X, Shi J, Yan M and Zhou T. Origins and evolving functionalities of tRNA-derived small RNAs. Trends Biochem Sci 2021; 46: 790-804.

[12] Liu B, Cao J, Wang X, Guo C, Liu Y and Wang T. Deciphering the tRNA-derived small RNAs: origin, development, and future. Cell Death Dis 2021; 13: 24.

[13] Lan S, Liu S, Wang K, Chen W, Zheng D, Zhuang Y and Zhang S. tRNA-derived RNA fragment, tRF-18-8R6546D2, promotes pancreatic adenocarcinoma progression by directly targeting ASCL2. Gene 2024; 927: 148739.

[14] Hu F, Niu Y, Mao X, Cui J, Wu X, Simone CB 2nd, Kang HS, Qin W and Jiang L. tsRNA-5001a promotes proliferation of lung adenocarcinoma cells and is associated with postoperative recurrence in lung adenocarcinoma patients. Transl Lung Cancer Res 2021; 10: 3957-3972.

[15] Han L, Lai H, Yang Y, Hu J, Li Z, Ma B, Xu W, Liu W, Wei W, Li D, Wang Y, Zhai Q, Ji Q and Liao T. A 5'-tRNA halve, tiRNA-Gly promotes cell proliferation and migration via binding to RBM17 and inducing alternative splicing in papillary thyroid cancer. J Exp Clin Cancer Res 2021; 40: 222.

[16] Crew KD and Neugut AI. Epidemiology of gastric cancer. World J Gastroenterol 2006; 12: 354-362.

[17] Bornschein J, Leja M, Kupcinskas J, Link A, Weaver J, Rugge M and Malfertheiner P. Molecular diagnostics in gastric cancer. Front Biosci (Landmark Ed) 2014; 19: 312-338.

[18] Balatti V, Nigita G, Veneziano D, Drusco A, Stein GS, Messier TL, Farina NH, Lian JB, Tomasello L, Liu CG, Palamarchuk A, Hart JR, Bell C, Carosi M, Pescarmona E, Perracchio L, Diodoro M, Russo A, Antenucci A, Visca P, Ciardi A, Harris CC, Vogt PK, Pekarsky Y and Croce CM. tsRNA signatures in cancer. Proc Natl Acad Sci U S A 2017; 114: 8071-8076.

[19] Zhu L, Li J, Gong Y, Wu Q, Tan S, Sun D, Xu X, Zuo Y, Zhao Y, Wei YQ, Wei XW and Peng Y. Exosomal tRNA-derived small RNA as a promising biomarker for cancer diagnosis. Mol Cancer 2019; 18: 74.

[20] Yang W, Gao K, Qian Y, Huang Y, Xiang Q, Chen C, Chen Q, Wang Y, Fang F, He Q, Chen S, Xiong J, Chen Y, Xie N, Zheng D and Zhai R. A novel tRNA-derived fragment AS-tDR-007333 promotes the malignancy of NSCLC via the HSPB1/MED29 and ELK4/MED29 axes. J Hematol Oncol 2022; 15: 53.

[21] Burger K, Schlackow M and Gullerova M. Tyrosine kinase c-Abl couples RNA polymerase II transcription to DNA double-strand breaks. Nucleic Acids Res 2019; 47: 3467-3484.

[22] Chen Q, Yan M, Cao Z, Li X, Zhang Y, Shi J, Feng GH, Peng H, Zhang X, Zhang Y, Qian J, Duan E, Zhai Q and Zhou Q. Sperm tsRNAs contribute to intergenerational inheritance of an acquired metabolic disorder. Science 2016; 351: 397-400.

[23] Park J, Ahn SH, Shin MG, Kim HK and Chang S. tRNA-derived small RNAs: novel epigenetic regulators. Cancers (Basel) 2020; 12: 2773.

[24] Fu BF and Xu CY. Transfer RNA-derived small RNAs: novel regulators and biomarkers of cancers. Front Oncol 2022; 12: 843598.

[25] Jin K, Wu J, Yang J, Chen B, Xu J, Bao H, Zong W, Xie C, Chen L and Wang F. Identification of serum tsRNA-Thr-5-0015 and combined with AFP and PIVKA-II as novel biomarkers for hepatocellular carcinoma. Sci Rep 2024; 14: 28834.

[26] Xu W, Zheng J, Wang X, Zhou B, Chen H, Li G and Yan F. tRF-Val-CAC-016 modulates the transduction of CACNA1d-mediated MAPK signaling pathways to suppress the proliferation of gastric carcinoma. Cell Commun Signal 2022; 20: 68.

[27] Zhang S, Gu Y, Ge J, Xie Y, Yu X, Wu X, Sun D, Zhang X, Guo J and Guo J. tRF-33-P4R8Y-P9LON4VDP inhibits gastric cancer progression via modulating STAT3 signaling pathway in an AGO2-dependent manner. Oncogene 2024; 43: 2160-2171.

[28] Xiong Q, Zhang Y, Xu Y, Yang Y, Zhang Z, Zhou Y, Zhang S, Zhou L, Wan X, Yang X, Zeng Z, Liu J, Zheng Y, Han J and Zhu Q. tiRNA-Val-CAC-2 interacts with FUBP1 to promote pancreatic cancer metastasis by activating c-MYC transcription. Oncogene 2024; 43: 1274-1287.

[29] Tao EW, Wang HL, Cheng WY, Liu QQ, Chen YX and Gao QY. A specific tRNA half, 5'tiRNA-His-GTG, responds to hypoxia via the HIF1α/ANG axis and promotes colorectal cancer progression by regulating LATS2. J Exp Clin Cancer Res 2021; 40: 67.

[30] Liang Y, Ji D, Ying X, Ma R and Ji W. tsRNA modifications: an emerging layer of biological regulation in disease. J Adv Res 2025; 74: 403-414.

[31] Xu R, Du A, Deng X, Du W, Zhang K, Li J, Lu Y, Wei X, Yang Q and Tang H. tsRNA-GlyGCC promotes colorectal cancer progression and 5-FU resistance by regulating SPIB. J Exp Clin Cancer Res 2024; 43: 230.

[32] Ying X, Hu W, Huang Y, Lv Y, Ji D, Chen C, Yang B, Zhang C, Liang Y, Zhang H, Liu M, Yuan G, Wu W and Ji W. A novel tsRNA, m7G-3' tiRNA LysTTT, promotes bladder cancer malignancy via regulating ANXA2 phosphorylation. Adv Sci (Weinh) 2024; 11: e2400115.